



Immune checkpoint expression on HIV-specific CD4+ T cells and response to their blockade are dependent on lineage and function

Elsa Brunet-Ratnasingham,^{a,b} Antigoni Morou,^{a,b,1} Mathieu Dubé,^a Julia Niessl,^{a,b,2} Amy E. Baxter,^{a,b,3} Olivier Tastet,^a Nathalie Brassard,^a Gloria Ortega-Delgado,^a Roxanne Charlebois,^a Gordon J. Freeman,^c Cécile Tremblay,^{a,b} Jean-Pierre Routy,^d and Daniel E. Kaufmann^{a,b*}

^aResearch Centre of the Centre Hospitalier de l'Université de Montréal (CRCHUM), Montreal, Quebec, Canada

^bUniversité de Montréal, Montreal, Quebec, Canada

^cDepartment of Medical Oncology, Dana-Farber Cancer Institute, Harvard Medical School, Boston, USA

^dChronic Viral Illnesses Service and Division of Hematology, McGill University Health Centre, Montreal, Quebec, Canada

Summary

Background Immune checkpoint blockade (ICB) partially reverses the dysfunctional state of antigen-specific T cell in chronic infections. However, its impact on the diverse subsets of CD4+ T cells in humans is largely unknown.

Methods We examined immune checkpoint (IC) expression and function in HIV-specific CD4+ T cells of viremic individuals (≥ 5000 vRNA cp/ml, $n = 17$) prior to ART and persons with spontaneous ($n = 11$) or therapy-induced ($n = 16$) viral suppression (< 40 cp/ml). We investigated IC patterns associated with exhaustion-related transcription factors and chemokine receptors using activation-induced marker assays. We determined effector functions representative of T_{FH}, T_{HI}, and T_{HI17}/T_{HI22} using RNA flow cytometric fluorescence in situ hybridization (FISH). We compared increase in cytokine expression upon ICB across functions and patient status.

Findings Expression of dysfunction-related molecules, such as transcription factors and ICs PD-1, TIGIT, and CD200, followed a hierarchy associated with infection status and effector profile. *In vitro* responsiveness to PD-1 blockade varied with defined functions rather than IC levels: frequencies of cells with T_{HI}- and T_{HI17}/T_{HI22}-, but not T_{FH}-related functions, increased. Cells co-expressing T_{HI} and T_{FH} functions showed response to ICB, suggesting that the cell's state rather than function dictates responsiveness to PD-1 blockade. Response to PD-1 blockade was strongest in viremic participants and reduced after ART initiation.

Interpretation Our data highlight a polarization-specific regulation of IC expression and differing sensitivities of antigen-specific T helper subsets to PD-1-mediated inhibition. This heterogeneity may direct and constrain ICB efficacy in restoring CD4+ T cell function in HIV infection and other diseases.

Funding NIH, CIHR, CFI, FRQS

Copyright © 2022 The Author(s). Published by Elsevier B.V. This is an open access article under the CC BY-NC-ND license (<http://creativecommons.org/licenses/by-nc-nd/4.0/>)

Keywords: HIV-specific CD4+ T cells; T cell dysfunction; Immune checkpoint blockade; PD-1; TOX; CD4+ T cell subsets

eBioMedicine 2022;84:
104254
Published online xxx
<https://doi.org/10.1016/j.ebiom.2022.104254>

*Corresponding author.

E-mail address: daniel.kaufmann@umontreal.ca (D.E. Kaufmann).

¹ Current affiliation: Roche Diagnostics, Penzberg, Bavaria, Germany.

² Current affiliation: Center for Infectious Medicine, Department of Medicine Huddinge, Karolinska Institutet, Stockholm, Sweden.

³ Current affiliation: Perelman School of Medicine, University of Pennsylvania, Philadelphia, USA

Research in context

Evidence before this study

Combination antiretroviral therapy (ART) is highly effective in controlling HIV but requires life-long medication due to the latent viral reservoir and does not restore suppressive immunity. There is no generation of effective HIV-specific T cell responses, which are thought to play an important role in controlling HIV in the rare individuals who can spontaneously control the virus. Inhibitory immune checkpoints (IC) such as PD-1 contribute to T cell dysfunction and failure to control viral infections, including HIV, and IC blockade (ICB) has been considered a potential adjuvant to ART through restoration of T cell functions and latency reversal of viral reservoirs. While most human studies have focused on CD8+ T cells, increasing evidence shows that the remarkable impact of ICB therapy in a subset of cancer patients is enhanced by functional CD4+ T cell help, which can be directly affected by ICB. While effective virus-specific CD4+ T cell responses are also thought to be important for immune control of HIV, these cells are highly heterogeneous. How IC expression and function differs across CD4+ T cell lineages and the consequences of this diversity for IC blockade (ICB) strategies are still poorly understood.

Added value of this study

To compare various stages of immune dysfunction, we examined people living with HIV (PLWH) with different levels of viral control pre-ART (including elite controllers who spontaneously control virus) and followed a cohort longitudinally post-ART. A panel of assays characterizing the blood T_{FH}, T_{H1}, and T_{H17}/T_{H22} HIV-specific CD4+ T cell subsets revealed a hierarchy of IC (PD-1, TIGIT, CD200) and dysfunction-related transcription factor TOX expression that depends not only on the person's infection status but also on the subset. Response to blockade of the PD-1 pathway resulted in increased antiviral, cytotoxic, and mucosal-protective functions but did not affect T_{FH}-related functions, highlighting a subset-specific responsiveness. The type of cytokine increased following ICB was heterogeneous among patients, and most prominent in viremic participants. It was subdued but not abrogated in the setting of viral suppression, highlighting increased sensitivity to ICB in the setting of high antigen exposure.

Implications of all the available evidence

Our work reveals strong links between IC expression patterns and HIV-specific CD4+ T cell differentiation. These results highlight a subset-specific responsiveness to PD-L1 blockade, suggesting that this strategy may result in a skewed immune restoration with limited impact on T_{FH} function. They reveal a previously unrecognized impact of ICB on mucosal immunity-related CD4+ functions, which may impact the scope of potential applications for ICB in HIV infection. Our study

emphasizes the importance of considering the differentiation profile of the CD4+ T cells in studies of ICB blockade, as it may direct ICB efficacy in HIV infection and in other infectious and non-infectious chronic human diseases.

Introduction

CD4+ T helper (T_H) cells orchestrate the immune responses against pathogens^{1,2} and defects in T helper responses contribute to lack of viral immune control in HIV infection. This diverse cell population polarizes towards lineages characterized by expression of chemokine receptors and transcription factors (TF), and produce distinct sets of cytokines.³ Beyond the prototypical antiviral T_{H1} subset (characterized by IFN γ and IL-2 production and expression of CXCR3 and T-BET), HIV-specific CD4+ T cells also include mucosal-related T_{H17}/T_{H22} (expressing CCR6 and ROR γ T, with functions including production of IL-17 and IL-22) and B-cell helper T_{FH} (CXCR5+ and BCL-6+ in tissue, whose canonical cytokines are IL-21 and CXCL13), the proportions of which are differentially related to spontaneous viral control.⁴

In chronic infections such as HIV, sustained antigenic exposure and inflammation alter both CD4+ and CD8+ T cell function, impeding viral control. CD8+ T cell exhaustion follows a gradient enforced by epigenetic remodelling with limited reversibility.^{5,6} TOX is a central transcription factor (TF) involved in the development and maintenance of exhausted CD8+ T cells in mice⁷ and humans,⁸ although its role in human CD8+ T cells is not limited to exhaustion.⁹ Dysfunctional CD4+ T cells differ from exhausted CD8+ T cells in that they present prominent features of altered differentiation: loss of antiviral and mucosal-protective functions, with skewing towards a T follicular helper (T_{FH})-like profile.⁴ Little is known about TFs implicated in CD4+ T cell dysfunction, although some, increased in mice models, overlap with exhaustion-related TF.¹⁰ Another commonality between dysfunctional CD4+ and CD8+ T cells is the upregulation of inhibitory immune checkpoints (IC),¹¹ albeit with differences in IC hierarchy between the two subsets.^{10,12–14} IC have dual roles as physiologic regulators of T cell activation and mediators of exhaustion.¹⁵ PD-1 is the best characterized IC contributing to both HIV-specific CD4+ and CD8+ T cell dysfunction,¹⁶ and correlates with disease progression^{12,14} and loss of antiviral function.¹⁶

In some people, immune checkpoint blockade (ICB), in particular blockade of the PD-1 signalling pathway, can partially rescue CD8+ T cell exhaustion. The high inter-individual variability in responsiveness to ICB is at least in part due to the ratio of responsive over

non-responsive cells.^{17,18} A population of mildly exhausted CD8⁺ T cells, called “progenitor exhausted”, with stem-like properties and intermediate levels of PD-1, primarily respond to ICB,^{17,19,20} while terminally exhausted CD8⁺ T cells, with high PD-1 and Tim3⁺ expression, have poor response.²⁰ There is no straightforward association between PD-1 level on HIV-specific CD4⁺ T cells and responsiveness to ICB,¹⁴ underlining the need for more detailed investigations that have been hampered by the heterogeneity of T helper cells and the paucity of tools to identify them in an antigen-specific manner. While PD-1's effect on CD4⁺ T cell function *in vivo* was classically described as IL-2 inhibition,^{21,22} studies in animal and human chronic infections demonstrate a broader impact. PD-1 blockade enhanced IFN γ ⁺ T_{H1}-responses specific to *Mycobacterium tuberculosis* and CTL-related functions of CD4⁺ T cells in murine models²³ and patients undergoing ICB for cancer therapy.²⁴ PD-1 blockade moderately increased IFN γ secretion by SIV-specific CD4⁺ T in non-human primates.²⁵ These primates displayed replenished T_{H17} in the gut, improved gut integrity, and longer survival off therapy,^{26,27} although ICB did not lead to viral control in the absence of ART.²⁸ *In vitro*, PD-1 blockade enhanced HIV-specific CD4⁺ T cell proliferation as well as IFN γ , IL-2, IL-13, and IL-21 production.¹⁴ A murine model of chronic infection showed subset-specific responses to PD-1 blockade,²⁹ and studies in humans with cancer also suggest preferential expansion of certain subsets, although it was not demonstrated in an antigen-specific manner.³⁰

Here, we sought to understand the characteristics of dysfunctional HIV-specific CD4⁺ T cell which relate to their responses to ICB. We pinpoint a previously underappreciated heterogeneity of IC and exhaustion-related TF expression patterns across types of CD4⁺ T cells. We measure the capacity of multiple subsets of CD4⁺ T cells to respond to PD-1 blockade. By contrasting the phenotypic markers of dysfunction and the response to blockade, we observed a lineage-specific responsiveness to ICB, which was dependent on cell state rather than a specific function. Despite high PD-1 expression, some T helper subsets, such as circulating T_{FH}, do not respond to blockade of this pathway alone. This variable sensitivity of human CD4⁺ T cell populations to ICB will likely constrain the profile of immune restoration and is consistent with data from animal models. A greater understanding of ICB's impact on CD4⁺ T cells can foster better focusing of immunotherapeutic interventions.

Materials and methods

Study design & ethics

Leukaphereses were obtained from study participants at the Montreal General Hospital, Montreal, Canada or at

the Centre Hospitalier de l'Université de Montréal (CHUM) in Montreal, Canada. The study was approved by the respective IRBs (IRB CHUM: 17.335) and participants gave written informed consent prior to enrolment. Samples were collected between 2013 and 2019 as part of a multicentric study (MP-37-2018-4029). Subject characteristics are summarized in Table 1. Chronic Progressors (CP) had plasma viral loads of at least 5000 viral RNA copies/ml and were infected and off treatment for at least 3 months at the time of collection of the “Pre-ART” sample. Longitudinal “Post-ART” samples were collected in these same subjects, after at least 6 months on ART and with an undetectable viral load. Elite controllers (EC) had spontaneously controlled viremia (< 40 viral RNA copies/ml) in the absence of ART and infected/off treatment for at least 1 year. PBMCs were isolated by the Ficoll density gradient method and stored in gas phase of a liquid nitrogen tank in 90%FBS with 10% DMSO.

Antibodies

All antibodies are listed in Supplementary Tables 1-4. Antibodies are monoclonal and raised in mice. All antibodies were validated by manufacturer and titrated with biological and/or isotype controls. Antagonist antibodies targeting a specific inhibitory receptor, or their isotypic controls, were added into culture 15 min prior to stimulation. The PD-L1 blocking antibody clone 29E.2A3(31) or an isotypic control (IgG2b, clone MPC-11, BioXcell, # BE0086) were used for the RNA Flow-FISH and most delayed ICS assays. For the co-blockade assay, we used blocking antibodies from BMS currently in clinical trials for use against multiple types of cancer: the anti-PD-L1 antibody (BMS-936559)³² and the anti-TIGIT antibody (BMS-986207) (advanced solid tumours: NCT04570839; metastatic solid cancers: NCT02913313; NSCLC: NCT05005273; multiple myeloma: NCT04150965).

Activation-induced marker (AIM) assay

As previously described,⁴ cryopreserved peripheral blood mononuclear cells (PBMCs) were thawed and rested in cell culture media (RPMI supplemented with 10% Human AB serum and PenStrep – 50 U/ml of penicillin and 50 µg/ml of streptomycin) at 37°C for 3 hours at a density of 10M/ml in 24-well plates. 15 min prior to stimulation, CD40 blocking antibody (clone HB14, Miltenyi, cat #: 130-094-133) was added to each well at 0.5 µg/ml, as well as antibodies staining CXCR5, CXCR3 and CCR6. Cells were either left unstimulated or stimulated with overlapping peptide pools of HIV Gag (JPT, PM-HIV-Gag ULTRA), at a final concentration of 0.5 µg/ml/peptide. Alternatively, 1µg/ml of Staphylococcal Enterotoxin B (SEB, Toxin Technology) was used to stimulate the cells as a positive control.

Variable	Elite Controllers (EC) (n = 11)			Chronic Progressors (CP) (n = 17)			p value CP vs EC	ART treated (ART) (n = 16)			p value ART vs all	
	Median	lower IQR OR %	Higher IQR	Median	lower IQR OR %	Higher IQR		Median	lower IQR OR %	Higher IQR		
Age [years]	46	37.5	52.5	41	37	47	0.422	49	39.5	55	0.241	
Sex							0.076				0.224	
	Male	6	55%	15	88%			15	94%			
	Female	5	45%	2	12%			1	6%			
Ethnicity							ns				ns	
	Caucasian	8	73%	11	65%			10	59%			
	African	3	27%	5	29%			5	29%			
	Hispanic	0	0%	1	6%			0	0%			
	NA	0	0%	0	0%			1	6%			
Time since diagnosis [years]	16.4	10.1	19.3	10.3	1.9	13.4	0.125	12.7	4.0	20.5	0.48	
Time on ART at sampling [years]	NA	NA	NA	NA	NA	NA	NA	2.4	0.5	27.7	NA	
Time off ART [years]	NA	NA	NA	1.8	0.3	9.7	NA	NA	NA	NA	NA	
CD4/CD8 ratio	1.08	0.89	1.22	0.31	0.25	0.25	<0.001	0.55	0.43	1.05	0.367	
	CD4 count [cell/mm ³]	652.5	551.75	676.75	321	228	406	<0.001	628	456.5	682.75	0.011
	CD8 count [cell/mm ³]	510	389.75	656	1079	632	1198	0.027	919.5	651	1217.25	0.644
VL [vRNA copies/mL]												
	At time of sampling	<40	<40	<40	22959	14614	96873	<0.001	<40	<40	40	<0.001
	Nadir	<40	<20	<40	34229	15693	55674	<0.001	34229	13381	68516.5	0.13
Co-infection												
	HCV	0	0%	1	6%		>0.99	2	13%		>0.99	
	CMV	9	82%	16	94%		0.543	14	88%		>0.99	
	NA	2	18%	1	6%			1	6%		ns	

Table 1: Subject characteristics. Median values are shown, with interquartile range (IQR) for continuous variables, or percentages (%) for categorical values. *p* values are Mann-Whitney for continuous, or Chi² for categorical. Significant differences are bolded. *p* values for ART are a comparison of the ART group to the combined groups of EC and CP. Exhaustion-related transcription factor TOX correlates with PD-1 expression.

Cells were stimulated for 9 hours, collected, washed and stained with LIVE/DEAD™ Fixable Aqua Dead Cell Stain Kit (20 mins, 4°C; ThermoFisher, #L34965). After washing, cells were incubated with FcR block (10mins, 4°C; Miltenyi) then stained with a cocktail of surface markers (30 mins, 4°C; See panel in Supplementary Table 1). Washed cells were then fixed with 2% paraformaldehyde (PFA) for 20 mins at RT, then washed and resuspended in PBS-2% FBS for flow acquisition on a 5-laser LSRII (BD BioSciences). For experiments with intranuclear transcription factor staining, fixation and permeabilization were done using eBioscience™ Fcγ3/Transcription Factor Staining Buffer Set (cat#: 00-5523-00) following kit instructions: surface-stained cells were fixed with 1X Fixation/Permeabilization for 30 min at RT in the dark, then washed and resuspended in 1X Permeabilization buffer with intranuclear antibody cocktail for 1h at RT in the dark. Analysis was performed using FlowJo (Treestar, V10). Gates were set on the unstimulated controls.

Combined cytokine/chemokine mRNA-Flow-FISH and protein staining assays

As previously described,⁴ PBMCs were thawed and rested for 2-3 hours in 48-well plates at 5M in 0.5ml in cell culture medium. 15 min prior to stimulation, a PD-L1 blocking antibody (29E.2A3³¹) or an isotypic control (IgG2b, clone MPC-11, BioXcell, # BE0086) at a concentration of 10 µg/ml were added into culture, along with antibodies staining CXCR5, CXCR3, and CCR6. PBMCs were then either left unstimulated or were stimulated with an HIV Gag peptide pool (JPT) or SEB for 12 hours. After incubation, cells were stained with Fixable Viability Dye eFluor™ 506 (20 min, 4°C; eBioscience, # 65-0866-14) before labelling of surface markers with surface antibodies (30 min, 4°C; See panel in Supplementary Table 2). Samples were next subjected to the PrimeFlow RNA® assay (ThermoFisher) for specific mRNA detection in a 96-well plate as per manufacturer's instructions. All buffers and fixation reagents were provided with the kit, with the exception of flow cytometry staining buffer (PBS - 2% FBS). Briefly, after fixation and permeabilization, cytokine/chemokine mRNAs were labelled with one of five combinations of probes listed in Supplementary Table 3. The probes were each diluted 1:20 in probe diluent and hybridized to the target mRNA for 2 hr at 40°C. Samples were washed to remove excess probes and stored overnight in the presence of RNase inhibitor 1X (RNasin). Signal amplification was achieved by sequential 1.5 hr incubations at 40°C with the pre-amplification and amplification mixes. Amplified mRNA was labelled with fluorescently-tagged probes for 1 hr at 40°C. Samples were acquired on a BD LSRFortessa™. Analysis was performed using FlowJo (Treestar, V10). Gates were set on unstimulated controls (see Figure S3b). Net frequencies of HIV-specific responses were calculated

by subtracting the background expression (signal detected in the absence of exogenous stimulation) from the value measured after Gag antigen stimulation. HIV-specific responses were considered positive when the frequency obtained with Gag stimulation was at least twice that obtained in the absence of stimulation. Responses not meeting this criterion were characterized as undetectable.

Delayed Intracellular cytokine staining

As previously described,³³ thawed, rested PBMCs were either left unstimulated or were stimulated with an HIV Gag peptide pool (JPT) or SEB. After a 9h stimulation, 1.25 µg/ml of brefeldin A (BD GolgiPlug) was added to culture and cells were further incubated for 12 hours. Cells were collected, washed and stained with AquaVivid Viability dye (20 mins, 4°C). After washing, cells were incubated with FcR block (10mins, 4°C) then stained for cocktail of surface markers (30 mins, 4°C; see supplementary table 4 for panel). Cells were washed and fixed with Fixation Solution (eBioscience, #88-8824-00) for 15 mins at RT, following which they were washed and stained for intracellular proteins with 1X Permeabilization Buffer (eBioscience, #00-8333-56) (30 mins, 4°C). Cells were washed once more with 1X Permeabilization buffer, then with PBS - 2%FBS and acquired on the BD LSRFortessa. Analysis was performed using FlowJo (Treestar, V10). Gates were set on unstimulated controls.

qRT PCR analysis of HIV-specific CD4+ T cells

These data were collected in a previously published study.⁴ Briefly, AIM assay was conducted as previously explained and CD69+CD40L+CD4+ T cells were live-sorted on a FACS Aria cell sorter (BD BioSciences) equipped for handling of biohazardous material, operated at 70 pounds per square inch with a 70-um nozzle (for gating strategy, please refer to⁴) 5000 cells were collected directly into RLT lysis buffer (Qiagen) and vigorously vortexed before flash-freezing. Total RNA was purified using the RNeasy Plus Micro Kit (Qiagen). cDNA was synthesized using all RNA available (or 1-5 ng) with the High-Capacity Reverse Transcription Kit with RNase Inhibitor (Life Technologies) (250 C for 10 min, 370 C for 120 min, 850 C for 5 min). cDNA equivalent to 1000 sorted cells was subjected to gene-specific preamplification using Taqman Preamp MasterMix (Applied Biosystems) and 96 pooled TaqMan Assays (Applied Biosystems – for full panels, please refer to⁴) at final concentration 0.2X (95°C for 10 min, followed by 16 cycles of 95°C for 15 s and 60°C for 4 min). The preamplified cDNA was diluted 5-fold in DNA suspension buffer (Teknova) and was mixed with TaqMan Universal PCR Master mix (Life Technologies) and 20X GE sample loading reagent (Fluidigm). 20X Taqman assays were diluted 1:1 with 2X assay loading buffer (Fluidigm). Taqman assays mixtures were loaded

onto a primed 96.96 Dynamic Array chip (Fluidigm). The chip was loaded into the IFC Controller, where each sample was mixed with each assay in every possible combination. The chip was transferred in a Biomark (Fluidigm) for real-time PCR amplification and fluorescence acquisition using single probe (FAM-MGB, reference: ROX) settings and the default hot-start protocol with 40 cycles. Cycle thresholds (Ct) were calculated using the Fluidigm BioMark software.

Sample size estimation

All subjects meeting criteria and for whom we had sufficient material were analysed for CP and for EC. Sample size calculation was performed *a posteriori*: we calculated a sample size of 8 per group to ensure at least 80% power to detect at least 2.5 fold difference between the frequency of PD-1+ cells among Gag-specific CD4+ T cells of CP vs EC using 2-sided independent Wilcoxon-Mann-Whitney with 5% level of significance,³⁴ with the assumptions (based on data acquired thus far) that i) the mean and standard deviation of PD-1 expression (geometric mean fluorescent intensity – gMFI) of Gag-specific CD4+ T cells in CPs is of 1800 ± 850 group versus of 720 ± 240 in ECs, ii) PD-1 gMFI on Gag-specific CD4+ T cells follow an asymptotically normal distribution and iii) both groups must be of equal size. To reach a statistically significant difference between both cohorts, 8 CP and 8 EC would need to be analysed. Given that untreated cohorts are rare in Canada, as ART is easily accessible, we have analysed all CP and EC with sufficient samples in our biobank. This amounted to 11 EC and 17 CP. We also included 16 patients on ART, including all CP-post-ART samples available ($n = 8$) and a random selection of the remaining 8 subjects among available samples fitting selection criteria (Table 1, Figure 1a).

Analysis strategy

There was no randomisation nor blinding during experiments nor during analysis. While the status of an individual was known prior to analysis we minimized potential bias by pairing individuals from different groups among rounds of experiments and by using analysis templates to maintain consistency in flow cytometry gating.

Analysis of the qRT-PCR data obtained on the microfluidic platform was carried out using GenEx software (MultiD Analyses, version 6). Five endogenous control genes were included in the Fluidigm run and the stability of endogenous control genes across all experimental samples was evaluated applying the NormFinder algorithm⁵⁰ in GenEx. The mean expression of the most stable endogenous control genes was used for normalization and calculation of $-\Delta Ct$ values. Principal component analysis and biplots were created using the `prcomp` and `fviz_pca_biplot` functions in R programming language.

The techniques used to detect HIV-specific CD4+ T cells (FlowFISH, ICS) have differing levels of specificity (“noise”, specifically detection of cytokine mRNA+ cells, for example, in the absence of stimulation – i.e. background) and sensitivity (some cytokines are poorly captured). We therefore used for their analysis methods that are widely applied for flow cytometry data. When comparing the frequencies of detected Gag-specific cytokine+ CD4+ T cells, we reported all net responses, as it is relevant to also account for responses that are low or undetectable. However, where we considered the phenotype of Gag-specific CD4+ T cells, we excluded the cytokine mRNA+ cells whose frequency upon Gag stimulated was less than 2-fold over background to avoid potentially skewing the observed phenotype by features of background cells. For comparison of the fold changes upon PD-1 blockade, or when comparing the phenotype of Gag-specific CD4+ T cells, the data points with undetectable Gag-specific responses were excluded from statistical analysis.

Statistics

The type of statistical test is specified in the figure legends and summarized in supplemental Table 6. Given the size of the cohorts and the known large range of HIV-specific CD4+ T cell responses detected,⁴ we opted for conservative non-parametric tests. Mann-Whitney U test (MW) were performed on unpaired contrasts of interest (CP vs EC). If multiple MW were performed in a same panel, we first performed a Kruskal-Wallis (KW) test, then the MW corrected for multiple comparisons, either with the original FDR method of Benjamini and Hochberg (BH) (FDR at 5%) if variables were independent (for example, between mutually exclusive subsets), or with the corrected method Benjamini and Yekutieli (B-Y) if we could not assume independence of variables (for example, when considering cells expressing cytokines mRNA+ which could co-express multiple cytokines). In all instances of multiple corrections, the reported value in figures is the q value (i.e. the adjusted *p* value of the BH test). For the comparison of categorical values (demographics table, Table 1), we applied Fisher’s exact test, better suited than the χ^2 for our small sample sizes.

When the pairwise comparison of interest was between paired samples (for example, IgG vs aPD-1, PreART vs PostART), we performed Wilcoxon signed rank test. If we compared multiple pairs in one panel, we performed multiple Wilcoxon signed rank tests, with correction using the BH (FDR at 5%) if variables were independent, or BY if not.

For comparisons between more than two paired values (such as chemokine expression on Gag-specific AIM+ CD4+ T cells, TOX expression on subsets of AIM+ CD4+ T cells), we performed a Friedman test, with correction using the BH (FDR at 5%) if variables were independent, or BY if not. Subjects with missing data (for

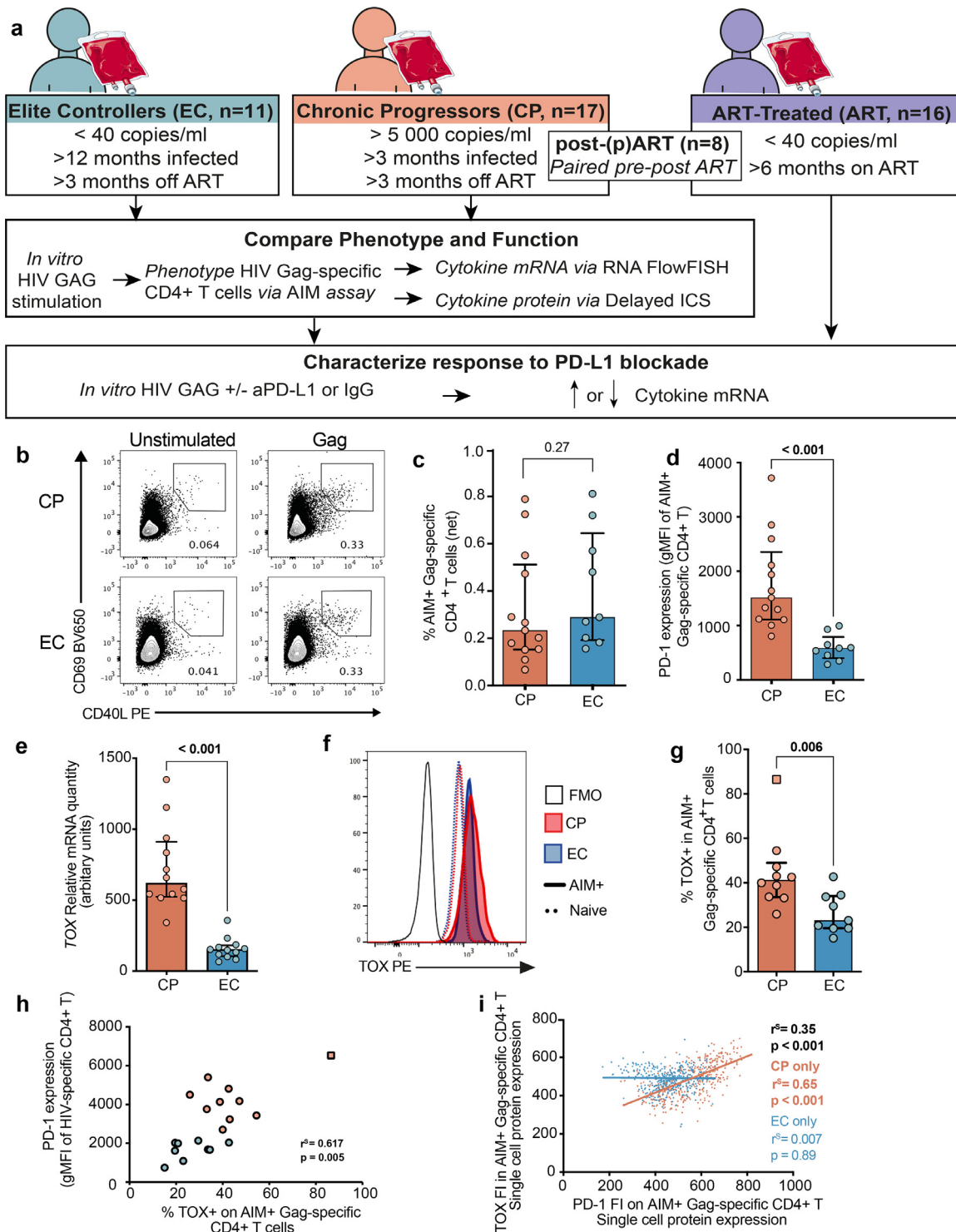


Figure 1. Increased expression of exhaustion-related transcription factors in HIV-specific CD4+ T cells of CP compared to EC.

a Flow chart of study design and main experiments. We studied three cohorts of HIV-infected individuals. Frozen PBMCs were thawed and stimulated with a peptide pool of HIV Gag. Gag-specific CD4+ T cells were then detected using either upregulation of activation induced marker (AIM) assay (for phenotyping) or via detection of cytokine mRNA (RNA FlowFISH) or protein (delayed ICS). To measure response to PD-L1 blockade (aPD-L1), PBMCs were stimulated in the presence of aPD-L1 or an isotypic control (IgG). Cytokine mRNA or protein were detected using aforementioned methods. **b** Representative flow cytometry plots of AIM+ Gag-

example, who had undetectable Gag-specific responses for one cytokine) were included in panels for representation purposes but excluded from statistical analysis.

Permutation test (10 000 permutations) was calculated using the SPICE software (<https://niaid.github.io/spice/>). All other statistical tests were performed with Prism v6.0 (GraphPad). Statistical tests were considered two-sided and $p < 0.05$ was considered significant. The heatmap, dendrogram and PCA were generated using the fold change between the net value of the frequency of a cytokine mRNA detected with PD-1 blockade over that seen for the same cytokine with the isotypic control. The prcomp function was used for the PCA, and the ggfortify and pheatmap packages were used for the dendrogram and heatmap, respectively. These packages, used within R, were solely utilized for representation purposes.

Role of funders

Funding agencies did not take part in study design, data collection, data analysis, interpretation or writing of results.

Results

Exhaustion-related transcription factor TOX correlates with PD-1 expression

To explore dysfunction among the heterogeneous T helper (T_H) populations, we compared dysfunctional HIV-specific CD4+ T cells from viremic chronic progressors with high viral burden prior to ART (CP; VL > 5000 viral RNA copies/ml) to the relatively functional HIV-specific CD4+ T cells from elite controllers who spontaneously suppress virus (EC; VL < 40 copies/ml) (patient characteristics in Table 1 and Study Flow Chart in Figure 1a).⁴ Upregulation of activation-induced markers (AIM) following peptide stimulation allows the capture of a broader antigen-specific CD4+ T cell population than cytokine-based techniques.³⁵ We stained for co-expression of CD69 and CD40L, an activation-induced co-signalling molecule expressed on multiple polarizations but low on bystander activated cells,^{4,35} after a 9-hour *ex vivo* stimulation with a peptide pool of HIV's immunodominant antigen, Gag (Figure 1b and

Figure 1a). Both cohorts had similar frequencies of AIM+ HIV-specific CD4+ T cells (Figure 1c), and PD-1 expression was higher on HIV-specific CD4+ T cells from CP than EC (Figure 1d, and Figure 1b), as previously reported.^{12,14}

We considered the exhaustion-related TF TOX, given its association with T cell exhaustion,⁷ and TFs reported in mouse dysfunctional CD4+ T cells¹⁰: Blimp-1 (Prdm1), Helios, Nfatc1, Batf, Eomes and Tbet. Our previously published high-throughput qRT-PCR assay data on sorted HIV-specific CD4+ T cells from CP or EC⁴ showed increased TOX (Figure 1e), IKZF2 (HELIOS), NFATC1, and PRDM1 (BLIMP-1) (Figure 1c) in HIV-specific CD4+ T cells of CP compared to EC, while BATF and TBX21 were higher in EC. EOMES was similar in both cohorts.

Selecting the TF increased CP compared to EC, we next performed intra-nuclear protein staining in HIV-specific CD4+ T cells using the 9h AIM assay (Figure 1d). HELIOS was undetectable in the AIM+ population, whereas both NFATC1 and TOX were increased in the CP compared to the EC (Figure 1d). TOX was most differential based on varying viral loads (Figure 1d). As CD4+ T cell dysfunction and viral load are strongly associated in HIV infection,⁴ TOX was best candidate for assessment of dysfunction by flow cytometry.

We set the TOX+ gate on naïve CD4+ T cells (Figure 1f) and confirmed a greater frequency of TOX+ cells in AIM+ HIV-specific CD4+ T cells of the CP cohort compared to EC (Figure 1g), while there was no difference in total CD4+ T cells between cohorts (Figure 1e). TOX showed a strong correlation with PD-1 expression at the patient level (Figure 1h), but a weak association at the single-cell level (Figure 1i). Of note, EC had a population of TOX+PD-1low cells not observed in CP (Figure 1g), abrogating the correlation between PD-1 and TOX single cell expression, while CP alone showed a strong single-cell correlation. These observations suggest TOX and PD-1 are increased jointly in the setting of dysfunction, perhaps from common upregulating signals.

Differential PD-1 expression in polarized HIV-specific CD4+ T cells

Among AIM+ HIV-specific CD4+ T cells, we characterized three polarizations based on chemokine-receptors

specific CD4+ T cells detection via upregulation of the activation-induced markers (AIM) CD69 and CD40L in a CP (top) and an EC (bottom) 9 hours after stimulation with a HIV Gag peptide pool. **c** Cumulative data of AIM+ Gag-specific CD4+ T cells per cohort [MW]. **d** Comparison of PD-1 expression on AIM+ HIV-specific CD4+ T cells in the CP (orange) and EC (blue) cohorts [MW]. **e** Relative *Tox* mRNA expression among sorted Gag-specific CD4+ T cells of CP (red) or EC (blue), as captured by high-throughput RT-PCR (Fluidigm® - for details, please see⁴ [MW]). **f** Representative example of TOX expression in AIM+ HIV-specific CD4+ T cells (shaded) or unstimulated naïve (CD45RA+CCR7+) CD4+T cells (dotted line) of both cohorts. Black line is FMO control. **g** Cumulative data of the frequency of TOX+ cells among AIM+ Gag-specific CD4+ T cells of CP (red) or EC (blue) [MW]. **h** Correlation between the frequency of TOX+ and PD-1 expression level among AIM+ Gag-specific CD4+ T cells [Sp]. **i** Correlation between the single cell expression (as captured by flow cytometry – FI = fluorescence intensity) of TOX and PD-1 on 100 cells per patient for 4 CP and 4 EC [Sp]. **cd** $n = 13$ CP and 9 EC. **e** $n = 9$ CP and 9 EC. **gh** $n = 10$ CP & 10 EC (only patients with detectable Gag shown). In **gh** statistical outlier (ROUT, $Q = 1\%$) identified by square shape; respective statistical tests remained highly significant with their exclusions. MW, Mann-Whitney U test; Sp, Spearman correlation.

expression: CXCR3, CCR6, and CXCR5, enriched on antiviral T_{HI} , mucosal-related T_{HI7}/T_{H22} , and B-cell helper T_{FH} , respectively (Figure 2a). Proportions were comparable between CP and EC, with the exception of a decreased CCR6+ fraction in CP (Figure S2a), as previously reported.⁴ TOX expression varied among polarizations and the hierarchy was not maintained between both cohorts: while in CP, the CXCR3+ polarization had significantly greater TOX levels than CCR6+ and CXCR5+, in EC TOX levels were greater in CCR6+ than CXCR5+, with a similar trend for CXCR3+ (Figure 2b).

PD-1 expression also varied among polarizations: highest PD-1 expression was again observed on CPs' CXCR3+, significantly greater than on CCR6+, with a similar trend for CXCR5+ (Figure 2cd). In EC, the hierarchy of PD-1 was similar to that of CP, but contrasted with the hierarchy of TOX in EC: CXCR3+ cells had the greatest PD-1 levels, although only significantly greater when compared to CCR6+ cells. This is in line with the absence of correlation for EC between single-cell expression PD-1 and TOX, and further emphasizes that PD-1 and TOX expression are specifically linked in the context of dysfunction.

CXCR3, CCR6, and CXCR5 can be co-expressed in various patterns, in line with the plastic nature of T_H (Figure 2eg). PD-1 expression was highest on the CXCR3+ CCR6- subsets for both cohorts (Figure 2fh, Supplementary Table 7). We further examined co-expression of classical "master" TFs with chemokine receptors, identifying T_{HI} as CXCR3+ T-BET+EOMES+, T_{HI7} as CCR6+ROR- γ t+CXCR3-, and T_{HI}/T_{HI7} as CCR6+ROR- γ t+CXCR3+ (Figure S2b).³⁶ T_{FH} 's master regulator BCL-6 was largely undetectable in peripheral CD4+ T cells (Figure S2b), as previously reported.³⁷ Among the AIM+ HIV-specific CD4+ T cells, the proportion of T_{HI7} was significantly higher in EC, with a similar trend for T_{HI}/T_{HI7} , while proportions of T_{HI} were similar (Figure S2c). PD-1 expression in CP always exceeded that in EC (Figure 2i) and, within both cohorts, T_{HI} cells had greater PD-1 expression than a CCR6+ polarization (Figure 2jk).

Thus, TOX and PD-1 expression follow similar patterns in the setting of dysfunction only; however, the differing hierarchy of PD-1 expression among subsets of HIV-specific CD4+ T cells is observed both in CP and in EC.

PD-1 levels differ according to HIV-specific CD4+ T cell functions

We further identified HIV-specific CD4+ T cell subsets by cytokine expression and cytotoxic functions. Flow cytometric RNA fluorescent *in situ* hybridization (RNA-Flow-FISH) assay can capture hard-to-detect cytokines transcribed by HIV-specific CD4+ T upon cognate antigen stimulation, with fluorescence intensity giving a semi-quantitative measurement of the number of RNA copies per cell.³⁸ We examined eight cytokines plus granzyme B (GZMB) that spanned five functional categories: IFN γ

and IL-2 for T_{HI} -associated functions; GZMB for cytotoxic activity; IL-22 and IL-17F for mucosal-related T_{HI7}/T_{H22} functions; IL-21, CXCL13, and IL-4 for T_{FH} -associated functions; and IL-10, a pleiotropic molecule with mostly inhibitory functions (Figure 3a, Figure S3a). CD69 served as a surrogate for recent activation to increase specificity for HIV antigen-induced cytokine mRNA (Figure S3b). HIV-specific CD4+ T cells producing *IL4* and *IL10* mRNA had low or undetectable frequencies in most participants and were not pursued (Figure S3bc). CPs had lower frequencies of *IL22* mRNA+ cells (Figure 3b), while amounts of transcripts did not differ significantly (Figure 3C). Conversely, CP exhibited a trend for increased frequencies of T_{FH} -related CXCL13 mRNA+ cells (Figure 3b). Polyfunctional cells were observed in both cohorts, with only the GZMB+*IL2*+ populations rarely detected (Figure S3d). The other combinations followed the expected trends (Figure S3d): *IL22* mRNA-expressing cells were greater in EC, whereas the CP had higher frequencies of all T_{FH} -related cytokines combinations. While the sizes of the cohorts were small for the T_{HI} -associated combinations, IFNG single-positive cells were the greatest population of all antiviral-related constellations among CP, consistent with the reported loss of polyfunctionality in HIV-specific T_{HI} .³⁹ Cytokine mRNA production following strong stimulation with the unspecific superantigen SEB showed no differences between the cohort (Figure S3e), suggesting that aforementioned differences are characteristics of HIV-specific CD4+ T cells.

Chemokine receptors expression among cytokine mRNA+ HIV-specific CD4+ T cells revealed complex associations between phenotype and function (Figure S3e). While CXCR3 was expressed on a large majority of GZMB, *IL2*, and IFNG mRNA+ cells, it was also present on most *IL21* and CXCL13 mRNA+ cells. A minority of T_{FH} -associated cytokine+ cells expressed CXCR5, with this proportion being smaller in CP. In contrast, almost all *IL22* or *IL17F* mRNA+ cells expressed CCR6.

Among defined T helper functions, PD-1's hierarchy was similar to that observed on chemokine-receptor-identified polarizations: low on cells producing GZMB and mucosal-associated cytokines *IL22* and *IL17F*; intermediate on T_{HI} (IFNG, *IL2*); high on T_{FH} (*IL21*, CXCL13) cytokine mRNA+ cells (Figure 3d-f, Supplementary Table 8). With the exception of low PD-1 on IFNG mRNA+ cells in EC, the hierarchy was similar in both cohorts (Figure 3ef).

These results demonstrate that HIV-specific CD4+ T cells can retain at least part of their functionality despite high PD-1 expression. Viremia leads to upregulation of this IC on functional cells, although the extent of its increase varies among T helper functions.

Differential responsiveness of individual cytokines to PD-1 blockade

Given the hierarchical expression of PD-1 among CD4+ T cells of different functions, we speculated that

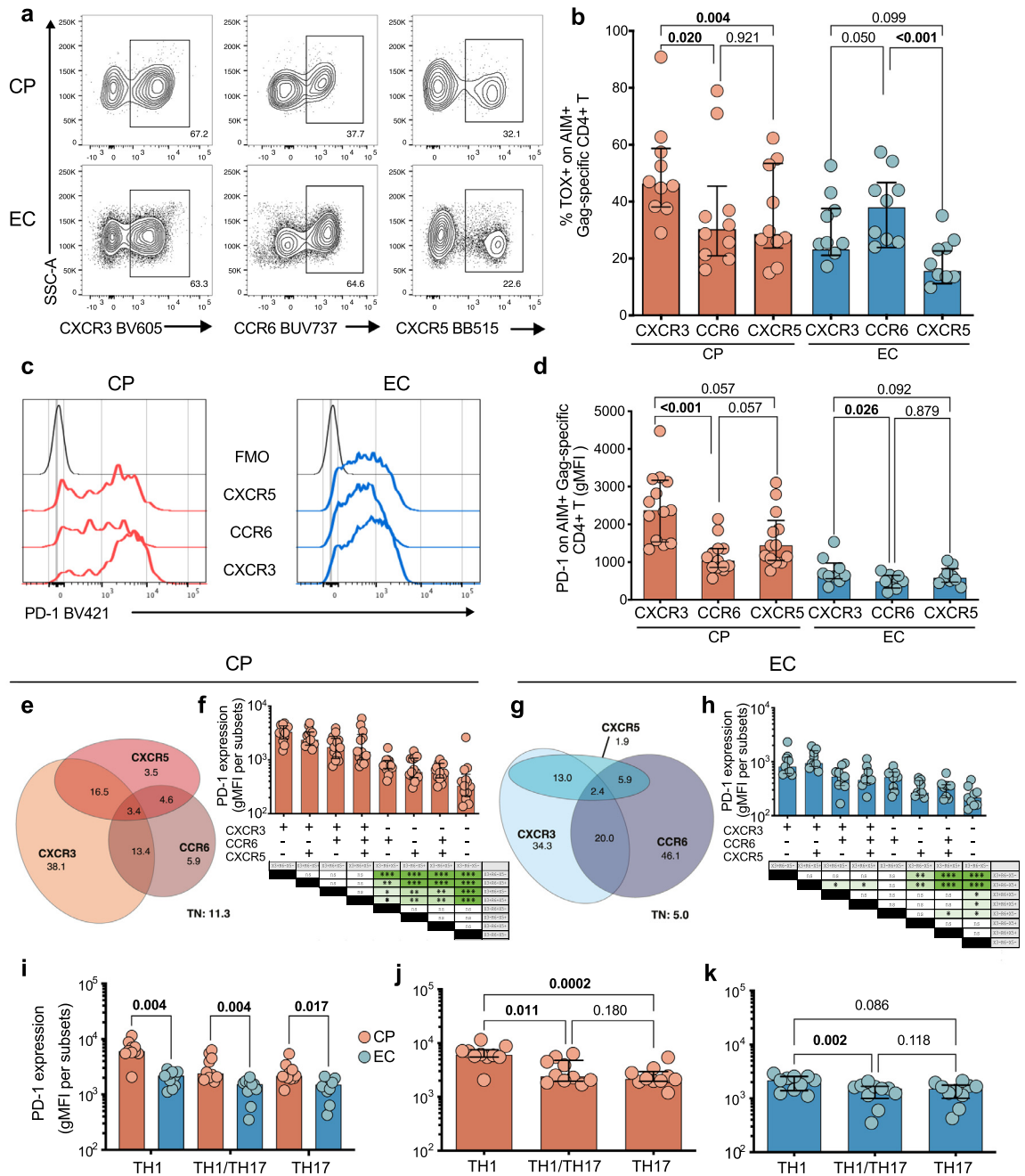


Figure 2. PD-1 expression on HIV-specific CD4+ T cells depends on their polarization. **a**) Representative flow cytometry plots of expression of the chemokine receptors CXCR3, CCR6 and CXCR5 on AIM+ Gag-specific CD4+ T cells of a CP (top) and an EC (bottom). **b**) Expression of TOX among chemokine-receptor-expressing Gag-specific CD4+ T cells among CP (red) or EC (blue) [Ft with BH]. **c**) Representative example and **d**) cumulative data of PD-1 expression among chemokine-receptor-expressing Gag-specific CD4+ T cells [Ft with BH]. Euler graphs of co-expression for CXCR3, CCR6, and CXCR5 on AIM+ Gag-specific CD4+ T cells in **e**) CP or **g**) EC. Values represent median frequencies of subsets within AIM+ Gag-specific CD4+ T cells. TN: negative for all three chemokine receptors. PD-1 expression in subsets of AIM+ Gag-specific CD4+ T cells subsets, as identified by chemokine co-expression patterns in **f**) CP [Ft with BY] or **h**) EC [Ft with BY]. PD-1 expression on CD4+ T cell subsets identified by chemokine receptor and master transcription factors, i) in CP vs EC [MW with BH], or between polarizations of **j**) CP [Ft with BY] or **k**) EC [Ft with BY]. In **b**) $n = 10$ CP and 10 EC; **df**) $n = 13$ CP and 9 EC; **ijk**) $n = 10$ CP and 10 EC. Columns correspond to median values, and whiskers, interquartile ranges. Adjusted p values are shown. **fh**) p values resulting from the comparison of PD-1 gMFI among subsets appear in tables below, with p values < 0.05 highlighted in green. $p > 0.5 = ns$; $p < 0.05 = *$; $p < 0.01 = **$; $p < 0.001 = ***$. Ft, Friedman test; MW, Mann Whitney U test; BH, Original FDR method of Benjamini and Hochberg (one per cohort); BY, Corrected method of Benjamini and Yekutieli; gMFI, Geometric Mean of Fluorescence Intensity.

responsiveness of these cells to blockade of PD-L1, the major ligand for PD-1 in PBMCs, would be heterogeneous as well. On cells from CP, PD-L1 blockade increased frequencies of HIV-specific cytokine mRNA+ CD4+ T cells for mucosal and antiviral functions (Figure 4ab). *IL21* mRNA+ cells were also increased with blockade, but not *CXCL13* mRNA+ cells. Blockade in EC had a globally smaller impact on HIV-specific CD4+ T cells (Figure 4c), with trends for increased frequencies only detected for *IL2* and *IL22*. The magnitude of response to ICB, as measured by the fold change of cytokine with blockade, was significantly greater in CP for *IL17F*, with similar trends for *IL2*. Fold increases upon blockade of the 7 functions classified the participants relative to their cohort by unsupervised hierarchical clustering (Figure 4e), and principal component analysis (PCA) clearly depicts disease status as the main source of variation (Figure 4f). CP were heterogeneous in which type of cytokine-producing cells were increased upon blockade, suggesting PD-L1 blockade does not result in a consistent profile of response even for one same antigen specificity. Nearly all combinatory subpopulations increased in frequencies upon PD-L1 blockade in CP, with the notable exception of *CXCL13* mRNA+ cells (Figure 4ghi). EC had overall lower responses (Figure S4abc). For most constellations, there was at least a trend for greater response in CP than in EC in terms of fold change (Figure S4def), although the spread in our relatively small cohorts did not allow to rank responsiveness to PD-L1 blockade among subsets.

To study whether the effects observed on mRNA translated to protein, we performed delayed intracellular cytokine staining (d-ICS) following Gag stimulation. Extended stimulation before the addition of brefeldin A allows to capture the expression of both cytokines produced early, like IL-2 and IFN γ , as well as molecules induced later, namely *CXCL13* and IL-21.³³ IL-17F and IL-22 were not detectable (Figure S4g). Cytokine protein and cytokine mRNA expression robustly correlated for the IFN γ , IL-2, and *CXCL13*, but not for IL-21, whose low expression profile made it harder to gate (Figure S4h). Frequencies of IL-2+ HIV-specific CD4+ T cells were increased upon blockade, with a similar trend for IFN γ +, while there was no effect on *CXCL13*+ cells (Figure S4i), reflecting the lack of response to PD-L1 blockade seen at the mRNA level.

These data demonstrate a heterogeneous capacity of functionally distinct HIV-specific CD4+ T cells to respond to PD-L1 blockade at the transcriptional and translational level, including for polyfunctional cells.

IC co-expression on HIV-specific CD4+ T cells is lineage- and function- specific

To understand the low responsiveness to blockade seen in T_{FH}, we examined expression of the other ICs TIGIT

and CD200, also expressed on T_{FH} cells.⁴⁰ Similar to PD-1, expression of these IC was higher on AIM+ HIV-specific CD4+ T cells of CP than EC (Figure 5a-d), and showed a moderate positive correlation with viremia in CP (Figure S5a), demonstrating an association between antigen burden and their accumulation, as previously shown for PD-1¹⁶ and TIGIT.⁴¹ Single-cell expression of TIGIT and CD200 was strongly correlated with that of PD-1 (Figure 5ef), and less so with each other (Figure S5b). Almost half of AIM+ HIV-specific CD4+ T cells of CP co-expressed all three IC, whereas only a small fraction was triple-positive in EC (Figure 5g), in line with IC co-upregulation in conditions of elevated CD4+ T cell dysfunction.¹⁰ These IC varied according to subsets of HIV-specific CD4+ T cells (Figure S5cd). TIGIT was high on CXCR5+ cells and low on CCR6+ cells in both cohorts, and only high on the CXCR3+ of CP (Figure S5e). CD200 expression followed very similar patterns (Figure S5f). Consistently, IC expression differed between HIV-specific cytokine mRNA+ CD4+ T cells of CP, with high expression on *IL21*, *CXCL13*, and *IFNG*, with a similar trend for *IL2*+ mRNA+ cells, and low IC levels on *GZMB*, *IL17F*, and *IL22* mRNA+ cells (Figure 5hi, Supplementary Table 9). CD200 was undetectable on mucosal-related cytokine mRNA+ cells. These patterns were conserved in EC (Figure S5ef), with once again the exception of *IFNG* mRNA+ cells, on which TIGIT and CD200 levels were low. Thus, TIGIT and CD200 are highly expressed on HIV-specific CD4+ T cells producing IL-2 or T_{FH}-associated cytokines even in the absence of viremia, yet IC accumulate on other cytokine+ cells only in the setting of dysfunction, in particular for functions reduced in CP compared to EC.

Combined ICB strategies targeting different molecules can be more potent than single blockade.^{10,11} We examined the impact of two clinical-grade ICB antibodies developed for immunotherapy, the anti-PD-L1 antibody BMS-936559 and the anti-TIGIT antibody BMS-g86207-Ab (Bristol-Myers Squibb) using d-ICS, allowing us to multiplex the four cytokines IFN γ , IL-2, IL-21, and *CXCL13* (Figure S5g). Single TIGIT blockade did not increase cytokine+ responses for any of the functions studied (Figure S5g). While dual blockade tended to further increase responses to single PD-L1 blockade, responses were heterogeneous within the CP cohort: depending on the participant, we observed limited response to any blockade strategy (Figure S5h, left), detectable responses in the co-blockade condition only (Figure S5h, middle) or modest to no benefit of co-blockade compared to single PD-1 blockade (Figure S5h, right). Our data suggests co-blockade strategies may generate responses in a larger fraction of individuals than single blockade, although some subjects may remain unresponsive.

Because of the differential response of IFN γ and *CXCL13* to blockade, we compared its impact between monofunctional cells and the population co-expressing

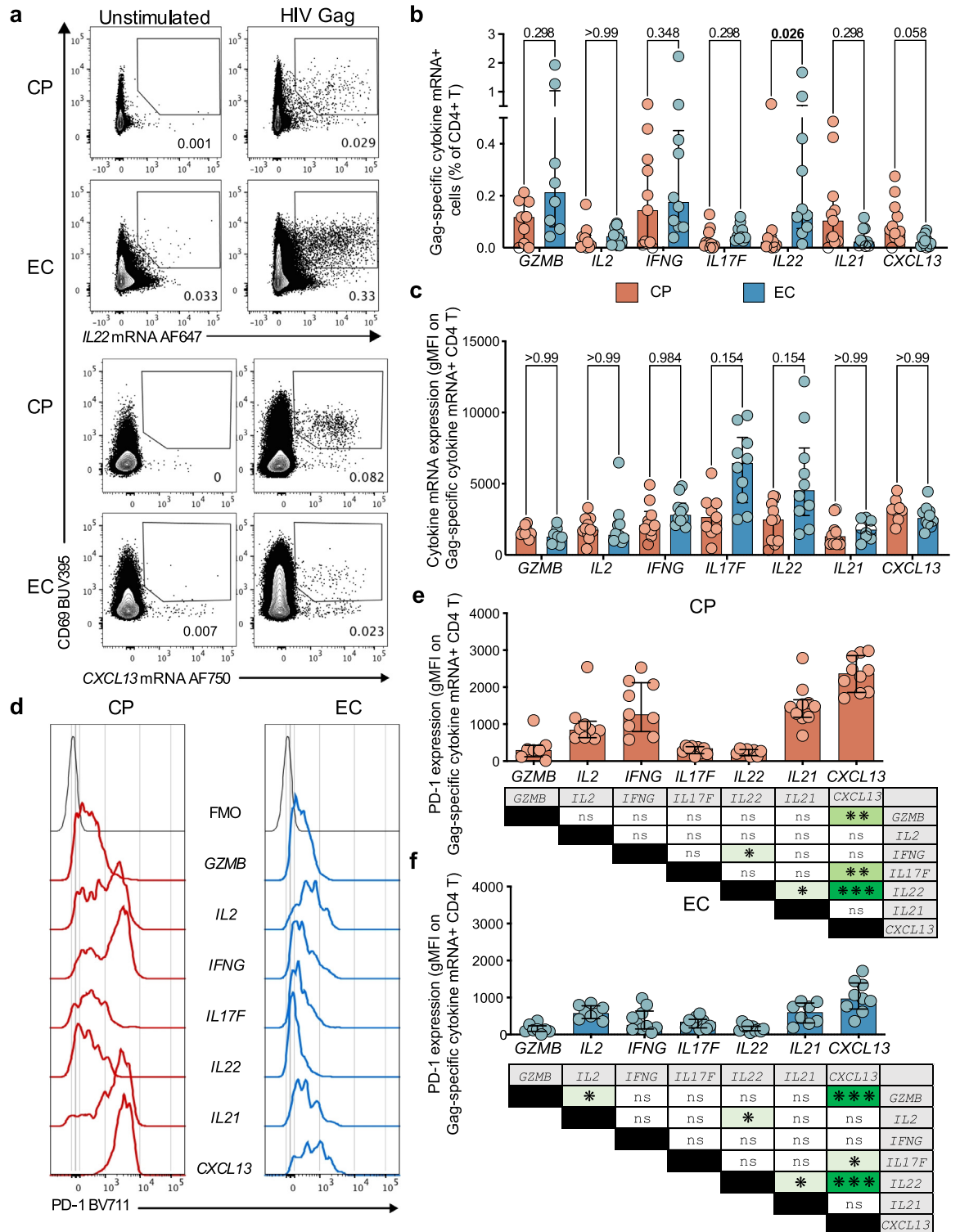


Figure 3. Heterogeneous PD-1 expression among cytokine-producing HIV-specific CD4+ T cells. **a**) Representative flow cytometry plots of *IL22* and *CXCL13* mRNA detection in a CP and an EC following a 12-hour stimulation with HIV Gag peptide pool. Cumulative data of the **b**) net frequencies [MW with BY] or **c**) cytokine mRNA gMFI of Gag-specific cytokine mRNA+ CD4+ T cells in both cohorts [MW with BY]. **d**) Representative examples and cumulative data of PD-1 expression on Gag-specific cytokine mRNA+ CD4+ T cells in **e**) CP [Ft with BY] or **f**) EC [Ft with BY]. *p* values resulting from the comparison of PD-1 gMFI among subsets appear in tables

CXCL13 and IFN γ , which represented roughly 20% of the overall cytokine-producing populations (Figure S5i). The frequency of IFN γ single-positive and or double-positive CD4⁺ T cells increased upon PD-L1 blockade, whereas CXCL13 single-positive cells remained refractory (Figure S5jk). The double-positive population also increased upon blockade, although only significant with co-blockade, highlighting that CXCL13 transcription can be susceptible to ICB.

These observations highlight the accumulation of ICs TIGIT and CD200 on subsets other than T_{FH} in the context of dysfunction. Despite harbouring the highest co-expression of TIGIT and PD-1, cells with TFH-related functions are refractory to dual TIGIT-PD-L1 blockade unless they co-express antiviral-associated functions.

ART-induced viral suppression differentially affects HIV-specific CD4⁺ T cell response to ICB

As ICB in HIV infection is predominantly being evaluated in ART-suppressed individuals in clinical settings, we measured the response to PD-L1 blockade among cells collected from PLWH treated with ART for at least 6 months. *IL2*, *IFNG*, and *IL21* were all significantly increased with blockade, with the strongest effect observed for *IL2* (Figure 6 a). While the differences in response to blockade were not sufficient to establish a clear hierarchy among most functions (Figure 6b), CXCL13 stood out as the only one significantly decreased upon blockade (Figure 6ab).

To see whether the level of responsiveness on suppressive ART compared to the responsiveness to PD-L1 blockade pre-ART, we compared responses in longitudinal samples obtained before and after ART initiation (Figure 6c, Figure S6a). The effect of ART was heterogeneous and subject-dependent, although the differences in median do suggest a decrease in T_{FH}-associated function, as described elsewhere⁴ (Figure 6d). Post-ART, there was a strong trend for decreased PD-1+ *IL21* and *CXCL13* mRNA+ CD4⁺ T cells (Figure S6b-d). These results highlight a correction of the high IC expression and T_{FH}-like skewing acquired in viremia towards a profile more similar to that observed in EC, while other functions are inconsistently recovered. When we compared the magnitude of response to PD-L1 blockade, there was no significant difference between time points, likely due to the high amount of variability and our small cohort size, although the increases for *IFNG* and mucosal-related cytokine expression to blockade were generally less pronounced after ART initiation, in line with the observations on the whole ART-treated cohort

(Figure 6e). No effect on the frequency of T_{FH}-cytokine+ CD4⁺ T cells was observed upon blockade during ART.

These data suggest that increased IL-2 and IFN γ production is a maintained benefit of PD-L1 blockade on ART, although their magnitude of response, as well as the impact on mucosal-related cytokines upon ICB may be reduced once ART is initiated.

Discussion

IC inhibit T cell activation through multiple mechanisms^{42,43}, for which the molecular features have been partially elucidated.^{5,43} However, most studies have been performed on CD8⁺ T cells and it is unclear whether IC operate differently among the heterogeneous lineages of CD4⁺ T cells. Using high-parameter flow cytometry combining protein and FISH mRNA staining, we assessed HIV-specific CD4⁺ T cells of an array of T helper phenotypes and functions otherwise difficult to measure. We focused on a palette of T_{FH}, T_{HI}, and T_{HI17}/T_{H22}-associated traits. These phenotypes, as identified by canonical chemokine receptors and transcription factors or by production of effector molecules, presented a hierarchy of relative expression levels of TOX, PD-1, TIGIT, and CD200. Among CD4⁺ T cell subsets, responsiveness to PD-L1 blockade varied according to function of rather than the levels of IC expression, with antiviral and mucosal-related functions responsive to ICB. While T_{FH}-related functions showed low reactivity to blockade, acquisition of T_{HI}-type functions rendered them responsive, suggesting that cell state rather than function was key. PD-L1 blockade had more limited effects in individuals with spontaneous or therapeutic control of viral replication than in people with high antigen load. These data highlight a previously unappreciated heterogeneity of responsiveness to ICB among HIV-specific CD4⁺ T cells and help understand the limited impact of ICB in HIV and SIV infections, particularly in the setting of therapeutically controlled viral load.

TOX expression was greater in HIV-specific CD4⁺ T cells of CP compared to EC, in line with their greater state of dysfunction linked with ongoing antigen stimulation in CP, and greater functionality in EC.⁴ TOX expression is linked to repeated TCR stimulation,^{7,44} a central driver of T cell exhaustion, and was strongly associated to PD-1 levels in the presence of viremia. Similar to TOX, HIV-specific CD4⁺ T cells from a same subject expressed different amounts of IC depending on their polarization, consistent across function-dependent (ICS) and function-agnostic (AIM) methods of identification. High expression or co-expression of IC

below, with p values < 0.05 highlighted in green. $p > 0.5 = \text{ns}$; $p < 0.05 = *$; $p < 0.01 = **$; $p < 0.001 = ***$. In bcef, $n = 11$ CP and 10 EC. In b) negative responses to Gag identified by grey shapes. In cef) only detectable responses are shown. Bars represent medians with interquartile range. Adjusted p values are shown. Ft, Friedman test; MW, Mann Whitney U test; BY, Corrected method of Benjamini and Yekutieli; gMFI, Geometric Mean of Fluorescence Intensity.

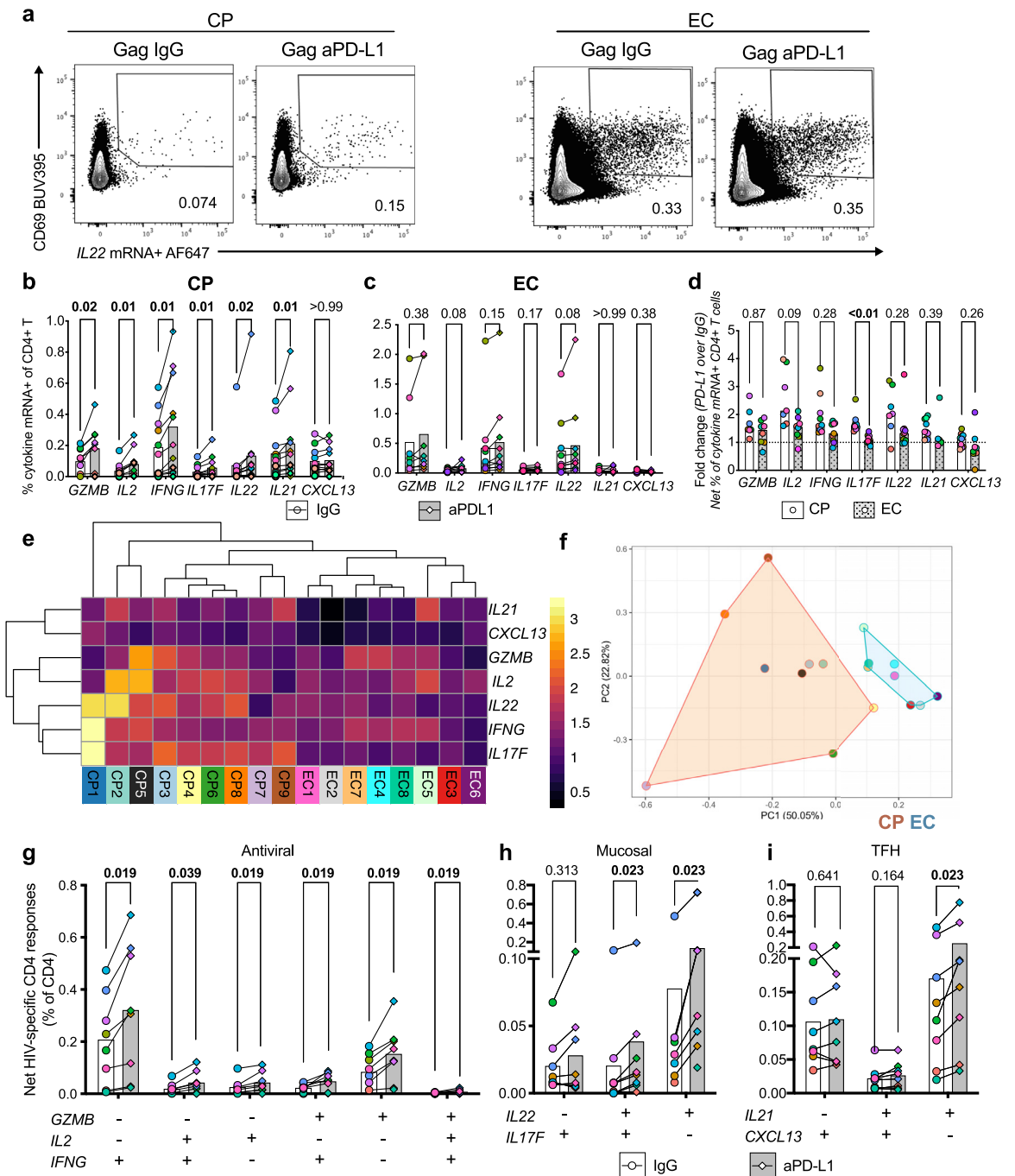


Figure 4. Differential responsiveness of individual HIV-specific CD4+ T cell cytokines to PD-1 blockade. **a** Representative flow cytometry plots of IL22 mRNA following Gag stimulation with PD-L1 blocking antibody (aPD-L1) or isotypic control (IgG) in a CP and an EC. Cumulative net frequency for all cytokine mRNA+ CD4+ T cells in **b** CP [mWx with BH] and **c** EC [mWx with BH]. **d** Fold change in the net frequencies of cytokine mRNA+ Gag-specific CD4+ T cells upon PD-L1 blockade compared to isotypic control for both cohorts [MW with BY]. **e** Unsupervised hierarchical clustering analysis and heatmap of fold changes per cytokine across subjects, with warmer colours representing stronger fold changes. Bottom row corresponds to individual subject IDs. **f** Principal component analysis (PCA) representation of CP and EC responses based on cytokine mRNA fold changes upon PD-L1 blockade. Red or blue shading regroups CP or EC, respectively. The numbers in parentheses are the percentage of variance explained by each principal component. Response of all cytokine mRNA combinations to PD-L1 blockade among CP, for the **g**) antiviral panel [mWx with BY]; **h**) mucosal panel [mWx with BY] or **i**) TFH panel [mWx with BY]. *n* = 11 CP and 9 EC. Columns correspond to median values with

did not prevent effector functions, as observed with IC-high CXCL13+, IL-2I+, and IL-2+ cells. T_{HO}/T_{TH1}-associated IL-2 markedly increased with PD-L1 blockade, consistent with an inhibitory effect by PD-1, while no effect was observed for T_{FH}-associated IL-2I and CXCL13. The hierarchy of IC expression between polarizations of HIV-specific CD4+ T cells suggest IC may not equally regulate the respective CD4+ T cell function. As shown in a TCR transfection model system of primary human PBMCs, some T cell functions are more resistant to PD-1-mediated inhibition than others,⁴⁵ while mouse and human T cell lines demonstrated different sensitivities of TCR-induced gene expression to PD-1 inhibition.⁴⁶ Recruited transcription factors as well as expression of co-stimulatory receptors can affect the sensitivity of a gene to PD-1,⁴⁶ both of which differ between T_{HI} and T_{FH}. Furthermore, IC may not be inhibitory in all instances: T_{FH} express lower amounts of IL-2I and IL-4 following PD-1 ablation in mice;⁴⁷ TIGIT, although inhibitory when expressed on CD8+ or T_{HI} T cells,^{48,49} is associated with strong B cell help and cytokine expression in T_{FH};⁵⁰ CD200 is associated with lack of pro-inflammatory cytokines, yet high IL-4 production in CD4+ T cells.⁵¹ Although these reports often find IC not inhibiting T_{FH}-related functions, our observation that CXCL13+IFN γ + cells increased in frequency upon ICB indicates this T_{FH} function can be negatively modulated by PD-1. Co-expression of CXCL13+ cells with a T_{HI}-associated cytokine may correspond to a plastic cell state which is responsive to ICB, while the absence of response in CXCL13 single-positive cells suggest that the response to blockade is associated with the cell-intrinsic state, rather than single cytokine pathways or IC expression.

Response to PD-L1 blockade was stronger in both breadth and magnitude for the dysfunctional HIV-specific CD4+ T cells of the CP compared to the EC and ART cohorts, suggesting that antigen presence sensitizes antigen-specific CD4+ T cells to ICB. Co-blockade with a TIGIT-blocking antibody further enhanced the effect of PD-L1 blockade only in some patients, consistent with the reported varying sensitivity to co-blockade among subjects,^{12,41,52} and highlighting the central inhibitory role of PD-1. Of note, HIV-specific CD4+T cells may respond directly to ICB by blockade of autologous PD-1 molecules, as we have shown with live-sorted CD4 T cells subsets and add back co-culture experiments,¹⁴ or indirectly by paracrine mechanisms, like the feed forward loop of soluble factors between T cells and antigen-presenting cells.⁵³ While their respective contributions would be extremely challenging to delineate on primary human T cells, the critical observation

remains that some subsets of HIV-specific CD4+ T cells are refractory to ICB at all levels of antigen exposure. While approaches combining immune checkpoint blockades have shown limited benefits in reinvigorating virus-specific CD4+ T cell function *in vitro*¹⁴ or viral control *in vivo*,²⁸ approaches combining ICB with other immune pathways may have synergistic effects.^{54,55}

Subset-specific refractiveness to PD-L1 blockade among virus-specific CD4+ T cells was recently observed in a murine model of chronic LCMV infection.²⁹ Thanks to the *in vivo* nature of the model, responses to ICB were amplified by proliferation, demonstrating increased T_{HI} and cytotoxic-type responses while T_{FH}-type responses were unaffected in CD4+ T cells from tissue,²⁹ in line with our results. Absence of response in cells with T_{FH}'s transcriptomic profile was also seen in mouse models of cancer.⁵⁶ However, these models did not permit study of mucosal-associated populations.

CD4+ T cells expressing mucosal cytokines responded well to PD-L1 blockade, despite the low levels of PD-1 expression on these cells overall. This suggests the replenished gut in the chronic SIV model may be linked to responsiveness of T_{HI17}/T_{H22} cells,^{26,27} the primary CD4+ T cell population of that anatomical site. In this scenario, bacteria-specific T_{HI17} may also have responded to ICB.⁵⁷ Taken together, our data suggests that polarizations nudging towards T_{HI} and T_{HI17} may undergo a more direct inhibition by PD-1, explaining their strong responsiveness to ICB. This can procure benefits such as improved gut integrity, even under conditions of persistent antigen, and highlight applications beyond viral control in HIV.

While ICB is not sufficient to control viral rebound,^{25–27} it is also considered for its latency-reversal potential: PD-L1 blockade increases viral production *in vitro*⁵⁸ and *in vivo*.^{59,60} In ART-treated PLWH, lymph node T_{FH} are key sources of inducible replication-competent virus.⁶¹ Our result has shown that these cells may not respond to ICB, highlighting the need for greater phenotypic characterization of reservoirs and of their ligands that can be exploited for viral reactivation. Indeed, blockade of PD-1 and CTLA-4 reactivate different reservoirs;²⁸ reactivation may benefit from combinatorial approaches targeting different reservoir subsets.

As rapid initiation of ART is now the standard of care upon HIV diagnosis, it is crucial to know whether the response to PD-L1 blockade changes once viremia is therapeutically suppressed. IL-2 increases upon blockade in all three cohorts, in line with the direct inhibitory role PD-1 plays in regulating this cytokine,²¹ although magnitude of response seemed decreased after ART

interquartile range as whiskers Each donor within a cohort has been separately colour coded. Adjusted *p* values are shown. mWx, multiple Wilcoxon tests; MW, Mann Whitney U test; BH, Original FDR method of Benjamini and Hochberg; BY, Corrected method of Benjamini and Yekutieli.

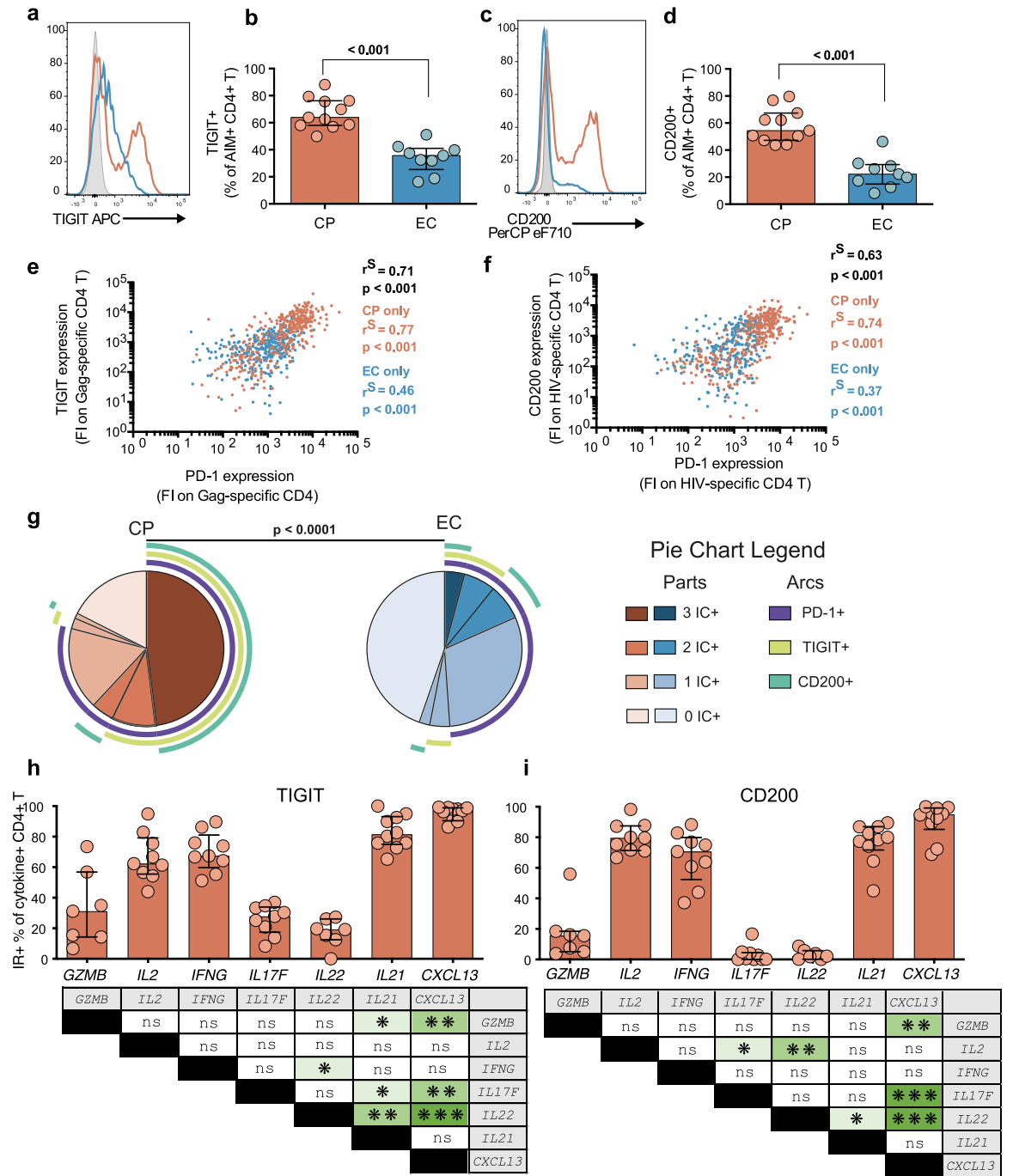


Figure 5. Differential expression of ICs among functionally distinct subsets of HIV-specific CD4+ T cells. Representative histogram overlays of **a**) TIGIT or **c**) CD200 expression on AIM+ Gag-specific CD4+ T cells from a CP (red) or an EC (blue). Grey shaded outline represents IC FMO. Fraction of AIM+ Gag-specific CD4+ T cells expressing **b**) TIGIT [MW] or **d**) CD200 of either cohort [MW]. Correlation [Sp] between single-cell expression of PD-1 and **e**) TIGIT or **f**) CD200 on AIM+ Gag-specific CD4+ T cells from 4 CP and 4 EC (100 cells per subject). **g**) Co-expression patterns between the ICs PD-1, TIGIT, and CD200 on AIM+ Gag-specific CD4+ T cells from both cohorts [Perm]. Shades of pie parts represent number of ICs; arcs represent IC expressed in pie part. Cumulative data of **h**) TIGIT [Ft with BY] and **i**) CD200 [Ft with BY] expression on cytokine mRNA+ Gag-specific CD4+ T cells from CP. Adjusted *p* values resulting from the comparison of frequency of IC among subsets appear in tables below, with *p* values < 0.05 highlighted in green. *p* > 0.5 = ns; *p* < 0.05 = *, *p* < 0.01 = **, *p* < 0.001 = ***, bdg) *n* = 13 CP and 9 EC; hi) *n* = 11 CP and 10 EC; only detectable Gag responses were considered. Columns and pie chart fractions correspond to median values, with whiskers as interquartile ranges. Perm, permutation test with 10 000 permutations; Ft, Friedman test; BY, Corrected method of Benjamini and Yekutieli; FI, Fluorescence Intensity.

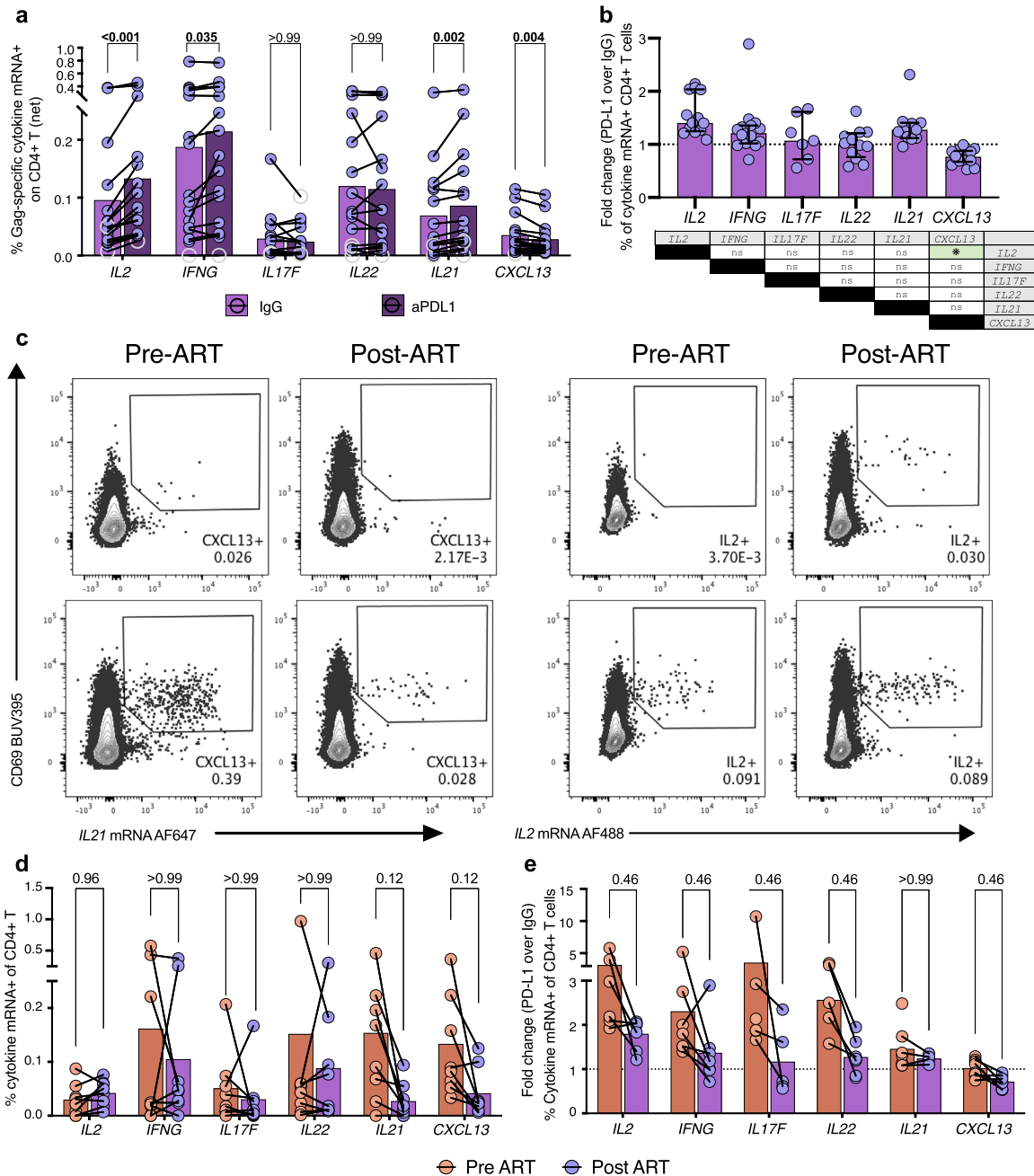


Figure 6. Viral suppression on ART differentially affects responsiveness of effector functions to PD-L1 blockade. a) Cumulative matched net frequencies of Gag-specific cytokine mRNA+ cells with PD-L1 blocking antibody compared to isotypic control (IgG) among ART cohort [mWx with BY]. **b)** Comparison of fold change among functions upon PD-L1 blockade in ART cohort [Ft with BY]. **c)** Representative examples and **d)** summary data of net frequency of Gag-specific cytokine mRNA+ CD4+ T cells from matched subjects prior to ART (red) and after ART (purple) [mWx with BY]. **e)** Comparison of the fold changes upon PD-L1 blockade between longitudinal samples pre- (red) and post-ART (purple) [mWx with BY]. ab) N = 16 ART. de) N = 8 longitudinal matched samples. Bars represent medians. mWx, multiple Wilcoxon tests; BY, Corrected method of Benjamini and Yekutieli; Ft, Friedman test. Adjusted *p* values are shown.

initiation. Responses of CD4+ T cells expressing IFN γ and mucosal-related cytokines to ICB also decreased in magnitude once ART was initiated. The general lowering of reactivity to ICB in contexts of controlled viremia strongly support a role of ongoing antigen presence in sensitizing these cells to this type of treatment. In addition, ART may block *de novo* generation of virus-specific CD4+ T cells, which may be more responsive to ICB.⁶² These observations are in line with studies in rhesus macaques, where ICB administration prior to ART initiation was more beneficial than when administered during ART,²⁷ highlighting the important role timing may play to maximize benefits of ICB in the context of HIV.

The demographics of the recruited cohorts in our study present some limitations. In line with the profile of the HIV-infected population in Montreal, the majority of the participants are male. Furthermore, for the viremic cohort, the individuals are recruited prior to initiation ART. Thus, they are often younger, explaining the age-gap between EC and CP. As this is a rare population, we were not able to include a more diverse population in terms of age and sex, and thus could not account for age and sex as confounding factors behind the observed differences. In addition, although more comprehensive than previous studies looking at HIV-specific CD4+ T cells, our observational study focused on a selected set of T helper functions. For example, we did not evaluate the effect of ICB on blocking the potentially inhibitory roles that HIV-specific CD4+ T cells can play, as described for CD4+ PD-1^{HI} cells in cancer murine models.⁵⁶

In summary, we highlight an intrinsic heterogeneity in IC expression among different polarizations of HIV-specific CD4+ T cells, revealing a disconnect between classical notions of IC and their relevance among CD4+ T cells lineages. Our data show different responses to ICB among functional lineages of HIV-specific CD4+ T cells, with CD4+ T cells expressing cytokines associated with mucosal immunity responding well, suggesting new therapeutic applications for ICB. In contrast, the absence of response among T_{FH}-associated cytokines suggests that ICB may not be used to increase TFH-assisted antibody maturation, and that these reservoir-harboring cells may reactivate poorly upon ICB. Finally, the decreased response to ICB in settings of controlled viremia suggest the ICB may be most beneficial prior to ART initiation, or in combination with treatment interruption strategies, which may constrain its applicability for HIV therapy. Our work emphasizes the importance of considering CD4+ T cell differentiation in studies of IC blockade in the context of T cell dysfunction, and with implications for other infectious and non-infectious chronic human diseases.

Contributors

Conceptualization: E.B.R., D.E.K., A.M., M.D.
Data Curation: E.B.R., A.M., J.N.

Data Verification: E.B.R., M.D., D.E.K.

Formal analysis: E.B.R., A.M., O.T., D.E.K.

Funding acquisition: D.E.K., M.D.

Investigation/experiments: E.B.R., A.M., N.B., G.O.D., R.C.

Methodology: E.B.R., A.M., J.N., A.E.B.

Resources: G.J.F., J.P.R., C.T.

Software: O.T.

Visualization: E.B.R., O.T.

Patient recruitment and cohort administration: N.B., C.T., J.P.R.

Supervision: D.E.K., A.M., M.D., A.E.B.

Writing – original draft: E.B.R., A.E.B., D.E.K.

All authors have read and approved the final version of the manuscript.

Data sharing statement

All data needed to understand the methodology, and evaluate the conclusions in the paper are present in the paper and/or the supplementary materials. We will consider sharing of data upon reasonable request (de-identified participant data only), this after signature of a material transfer agreement, up to 5 years following the publication of this article. The process for data transfer and access will be discussed according to the type of results requested and in a way that ensures integrity and practicality.

Declaration of interests

G.J.F. has patents/pending royalties on the PD-1/PD-L1 pathway from Roche, Merck M.S.D., Bristol-Myers-Squibb, Merck K.G.A., Boehringer-Ingelheim, AstraZeneca, Dako, Leica, Mayo Clinic, and Novartis. G.J.F. has served on advisory boards for Roche, Bristol-Myers-Squibb, Xios, Origimed, Triursus, iTeos, and NextPoint. G.J.F. has equity in Nextpoint, Triursus, and Xios. The anti-PD-L1 antibody BMS-936559 and the anti-TIGIT antibody BMS-g86207-Ab were given by Bristol-Myers Squibb. C.T. serves as a consultant and has received honoraria from Merck, Gilead, G.S.K., AstraZeneca and Medicago. None of aforementioned companies had implications in the design and interpretation of the experiments performed in this manuscript.

Acknowledgments

We thank Josée Girouard, the clinical staff at the McGill University Health Centre in Montreal and all study participants for their invaluable role in this project. We thank Alina Dyachenko, Justin Bélair and Raphaël Lima-Barbosa for help with statistical analyses. We also thank all funding agencies for their support: this study was supported by the National Institutes of Health (HL092565, to D.E.K.; R37AI112787 and P01AI056299 to G.J.F.); the Canadian Institutes for Health Research

(grants 137694 and 152977 to D.E.K.; grant MOP-93770 to C.T), Canada Foundation for Innovation Program Leader grants (grants #31756 and 37521 to D.E.K.), the FRQS AIDS and Infectious Diseases Network. D.E.K is a Merit Research Scholar of the Quebec Health Research Fund (FRQS). J.P.R is the holder of Louis Lowenstein Chair in Hematology & Oncology, McGill University. E. B. R. received a scholarship from the Faculté des Études Supérieures (FESP) of the Université de Montréal.

Supplementary materials

Supplementary material associated with this article can be found in the online version at doi:10.1016/j.ebiom.2022.104254.

References

- Laidlaw BJ, Craft JE, Kaech SM. The multifaceted role of CD4(+) T cells in CD8(+) T cell memory. *Nat Rev Immunol*. 2016;16(2):102–111.
- Swain SL, McKinstry KK, Strutt TM. Expanding roles for CD4(+) T cells in immunity to viruses. *Nat Rev Immunol*. 2012;12(2):136–148.
- Becattini S, Latorre D, Mele F, et al. T cell immunity. Functional heterogeneity of human memory CD4(+) T cell clones primed by pathogens or vaccines. *Science*. 2015;347(6220):400–406.
- Morou A, Brunet-Ratnasingham E, Dube M, et al. Altered differentiation is central to HIV-specific CD4(+) T cell dysfunction in progressive disease. *Nat Immunol*. 2019;20(8):1059–1070.
- Sen DR, Kaminski J, Barnitz RA, et al. The epigenetic landscape of T cell exhaustion. *Science*. 2016;354(6316):1165–1169.
- Pauken KE, Sammons MA, Odorizzi PM, et al. Epigenetic stability of exhausted T cells limits durability of reinvigoration by PD-1 blockade. *Science*. 2016;354(6316):1160–1165.
- Khan O, Giles JR, McDonald S, et al. TOX transcriptionally and epigenetically programs CD8(+) T cell exhaustion. *Nature*. 2019;571(7764):211–218.
- Heim K, Binder B, Sagar WD, et al. TOX defines the degree of CD8 + T cell dysfunction in distinct phases of chronic HBV infection. *Gut*. 2020;70(8):1550–1560.
- Sekine T, Perez-Potti A, Nguyen S, et al. TOX is expressed by exhausted and polyfunctional human effector memory CD8(+) T cells. *Sci Immunol*. 2020;5(49).
- Crawford A, Angelosanto JM, Kao C, et al. Molecular and transcriptional basis of CD4(+) T cell dysfunction during chronic infection. *Immunity*. 2014;40(2):289–302.
- Wherry EJ, Kurachi M. Molecular and cellular insights into T cell exhaustion. *Nat Rev Immunol*. 2015;15(8):486–499.
- Kaufmann DE, Kavanagh DG, Pereyra F, et al. Upregulation of CTLA-4 by HIV-specific CD4+ T cells correlates with disease progression and defines a reversible immune dysfunction. *Nat Immunol*. 2007;8(11):1246–1254.
- Kassu A, Marcus RA, D'Souza MB, et al. Regulation of virus-specific CD4+ T cell function by multiple costimulatory receptors during chronic HIV infection. *J Immunol*. 2010;185(5):3007–3018.
- Porichis F, Kwon DS, Zupkosky J, et al. Responsiveness of HIV-specific CD4 T cells to PD-1 blockade. *Blood*. 2011;118(4):965–974.
- Schildberg FA, Klein SR, Freeman GJ, Sharpe AH. Coinhibitory pathways in the B7-CD28 ligand-receptor family. *Immunity*. 2016;44(5):955–972.
- Day CL, Kaufmann DE, Kiepiela P, et al. PD-1 expression on HIV-specific T cells is associated with T-cell exhaustion and disease progression. *Nature*. 2006;443(7109):350–354.
- Kamphorst AO, Pillai RN, Yang S, et al. Proliferation of PD-1+ CD8 T cells in peripheral blood after PD-1-targeted therapy in lung cancer patients. *Proc Natl Acad Sci U S A*. 2017;114(19):4993–4998.
- Jiao S, Subudhi SK, Aparicio A, et al. Differences in tumor micro-environment dictate T helper lineage polarization and response to immune checkpoint therapy. *Cell*. 2019;179(5):1177–90 e13.
- Im SJ, Hashimoto M, Gerner MY, et al. Defining CD8+ T cells that provide the proliferative burst after PD-1 therapy. *Nature*. 2016;537(7620):417–421.
- Miller BC, Sen DR, Al Abosy R, et al. Subsets of exhausted CD8(+) T cells differentially mediate tumor control and respond to checkpoint blockade. *Nat Immunol*. 2019;20(3):326–336.
- Quigley M, Pereyra F, Nilsson B, et al. Transcriptional analysis of HIV-specific CD8+ T cells shows that PD-1 inhibits T cell function by upregulating BATF. *Nat Med*. 2010;16(10):1147–1151.
- Zuazo M, Arasanz H, Fernandez-Hinojal G, et al. Functional systemic CD4 immunity is required for clinical responses to PD-L1/PD-1 blockade therapy. *EMBO Mol Med*. 2019;11(7):e10293.
- Sakai S, Kauffman KD, Sallin MA, et al. CD4 T cell-derived IFN-gamma plays a minimal role in control of pulmonary mycobacterium tuberculosis infection and must be actively repressed by PD-1 to prevent lethal disease. *PLoS Pathog*. 2016;12(5):e1005667.
- Barber DL, Sakai S, Kudchadkar RR, et al. Tuberculosis following PD-1 blockade for cancer immunotherapy. *Sci Transl Med*. 2019;11(475):eaat2702. <https://doi.org/10.1126/scitranslmed.aat2702>.
- Velu V, Titanji K, Zhu B, et al. Enhancing SIV-specific immunity in vivo by PD-1 blockade. *Nature*. 2009;458(7235):206–210.
- Dyavar Shetty R, Velu V, Titanji K, et al. PD-1 blockade during chronic SIV infection reduces hyperimmune activation and microbial translocation in rhesus macaques. *J Clin Invest*. 2012;122(5):1712–1716.
- Mylvaganam GH, Chea LS, Tharp GK, et al. Combination anti-PD-1 and antiretroviral therapy provides therapeutic benefit against SIV. *JCI Insight*. 2018;3(18):e122940. <https://doi.org/10.1172/jci.insight.122940>.
- Harper J, Gordon S, Chan CN, et al. CTLA-4 and PD-1 dual blockade induces SIV reactivation without control of rebound after antiretroviral therapy interruption. *Nat Med*. 2020;26(4):519–528.
- Snell LM, Xu W, Abd-Rabbo D, et al. Dynamic CD4(+) T cell heterogeneity defines subset-specific suppression and PD-L1-blockade-driven functional restoration in chronic infection. *Nat Immunol*. 2021;22(12):1524–1537.
- Kagamu H, Kitano S, Yamaguchi O, et al. CD4(+) T-cell Immunity in the Peripheral Blood Correlates with Response to Anti-PD-1 Therapy. *Cancer Immunol Res*. 2020;8(3):334–344.
- Brown JA, Dorfman DM, Ma FR, et al. Blockade of programmed death-1 ligands on dendritic cells enhances T cell activation and cytokine production. *J Immunol*. 2003;170(3):1257–1266.
- Sunshine J, Taube JM. PD-1/PD-L1 inhibitors. *Curr Opin Pharmacol*. 2015;23:32–38.
- Niessl J, Baxter AE, Morou A, et al. Persistent expansion and Th-like skewing of HIV-specific circulating T follicular helper cells during antiretroviral therapy. *EBioMedicine*. 2020;54:102727.
- Shieh G, Jan S-I, Randles RH. On power and sample size determinations for the Wilcoxon–Mann–Whitney test. *Journal of Nonparametric Statistics*. 2006;18(1):33–43.
- Reiss S, Baxter AE, Cirelli KM, et al. Comparative analysis of activation induced marker (AIM) assays for sensitive identification of antigen-specific CD4 T cells. *PLoS One*. 2017;12(10):e0186998.
- O'Shea JJ, Paul WE. Mechanisms underlying lineage commitment and plasticity of helper CD4+ T cells. *Science*. 2010;327(5969):1098–1102.
- Locci M, Havenar-Daughton C, Landais E, et al. Human circulating PD-1+CXCR3-CXCR5+ memory Tfh cells are highly functional and correlate with broadly neutralizing HIV antibody responses. *Immunity*. 2013;39(4):758–769.
- Porichis F, Hart MG, Griesbeck M, et al. High-throughput detection of miRNAs and gene-specific mRNA at the single-cell level by flow cytometry. *Nat Commun*. 2014;5:5641.
- Vella LA, Herati RS, Wherry EJ. CD4(+) T cell differentiation in chronic viral infections: the Tfh perspective. *Trends Mol Med*. 2017;23(12):1072–1087.
- Sade-Feldman M, Yizhak K, Bjorgaard SL, et al. Defining T cell states associated with response to checkpoint immunotherapy in melanoma. *Cell*. 2018;175(4):998–1013 e20.
- Chew GM, Fujita T, Webb GM, et al. TIGIT Marks exhausted T cells, correlates with disease progression, and serves as a target for immune restoration in HIV and SIV infection. *PLoS Pathog*. 2016;12(1):e1005349.
- Chen L, Flies DB. Molecular mechanisms of T cell co-stimulation and co-inhibition. *Nat Rev Immunol*. 2013;13(4):227–242.
- Hui E, Cheung J, Zhu J, Su X, et al. T cell costimulatory receptor CD28 is a primary target for PD-1-mediated inhibition. *Science*. 2017;355(6332):1428–1433.
- Alfei F, Kanev K, Hofmann M, et al. TOX reinforces the phenotype and longevity of exhausted T cells in chronic viral infection. *Nature*. 2019;571(7764):265–269.

- 45 Wei F, Zhong S, Ma Z, et al. Strength of PD-1 signaling differentially affects T-cell effector functions. *Proc Natl Acad Sci U S A*. 2013;110(27):E2480–E2489.
- 46 Shimizu K, Sugiura D, Okazaki I, et al. PD-1 Imposes qualitative control of cellular transcriptomes in response to T cell activation. *Molecular Cell*. 2020;77(1):1–14.
- 47 Good-Jacobson KL, Szumilas CG, Chen L, Sharpe AH, Tomayko MM, Shlomchik MJ. PD-1 regulates germinal center B cell survival and the formation and affinity of long-lived plasma cells. *Nat Immunol*. 2010;11(6):535–542.
- 48 Tauriainen J, Scharf L, Frederiksen J, et al. Perturbed CD8+ T cell TIGIT/CD226/PVR axis despite early initiation of antiretroviral treatment in HIV infected individuals. *Sci Rep*. 2017;7:40354.
- 49 Joller N, Lozano E, Burkett PR, et al. Treg cells expressing the coinhibitory molecule TIGIT selectively inhibit proinflammatory Th1 and Th17 cell responses. *Immunity*. 2014;40(4):569–581.
- 50 Godefroy E, Zhong H, Pham P, Friedman D, Yazdanbakhsh K. TIGIT-positive circulating follicular helper T cells display robust B-cell help functions: potential role in sickle cell alloimmunization. *Haematologica*. 2015;100(11):1415–1425.
- 51 Caserta S, Nausch N, Sawtell A, et al. Chronic infection drives expression of the inhibitory receptor CD200R, and its ligand CD200, by mouse and human CD4 T cells. *PLoS One*. 2012;7(4):e35466.
- 52 Grabmeier-Pfistershammer K, Stecher C, Zettl M, et al. Antibodies targeting BTLA or TIM-3 enhance HIV-1 specific T cell responses in combination with PD-1 blockade. *Clin Immunol*. 2017;183:167–173.
- 53 Porichis F, Hart MG, Zupkosky J, et al. Differential impact of PD-1 and/or interleukin-10 blockade on HIV-1-specific CD4 T cell and antigen-presenting cell functions. *J Virol*. 2014;88(5):2508–2518.
- 54 Tsukamoto H, Fujieda K, Miyashita A, et al. Combined blockade of IL6 and PD-1/PD-L1 signaling abrogates mutual regulation of their immunosuppressive effects in the tumor microenvironment. *Cancer Res*. 2018;78(17):5011–5022.
- 55 Goshu BA, Chen H, Moussa M, Cheng J, Catalfamo M. Combination rhIL-15 and anti-PD-L1 (Avelumab) enhances HIVGag-Specific CD8 T-Cell function. *J Infect Dis*. 2020;222(9):1540–1549.
- 56 Zappasodi R, Budhu S, Hellmann MD, et al. Non-conventional Inhibitory CD4(+)Foxp3(-)PD-1(hi) T cells as a biomarker of immune checkpoint blockade activity. *Cancer Cell*. 2018;33(6):1017–32 e7.
- 57 Perreau M, Vigano S, Bellanger F, et al. Exhaustion of bacteria-specific CD4 T cells and microbial translocation in common variable immunodeficiency disorders. *J Exp Med*. 2014;211(10):2033–2045.
- 58 Fromentin R, DaFonseca S, Costiniuk CT, et al. PD-1 blockade potentiates HIV latency reversal ex vivo in CD4(+) T cells from ART-suppressed individuals. *Nat Commun*. 2019;10(1):814.
- 59 Guihot A, Marcelin AG, Massiani MA, et al. Drastic decrease of the HIV reservoir in a patient treated with nivolumab for lung cancer. *Ann Oncol*. 2018;29(2):517–518.
- 60 Scully EP, Rutishauser RL, Simoneau CR, et al. Inconsistent HIV reservoir dynamics and immune responses following anti-PD-1 therapy in cancer patients with HIV infection. *Ann Oncol*. 2018;29(10):2141–2142.
- 61 Perreau M, Savoye AL, De Crignis E, et al. Follicular helper T cells serve as the major CD4 T cell compartment for HIV-1 infection, replication, and production. *J Exp Med*. 2013;210(1):143–156.
- 62 Snell LM, Osokine I, Yamada DH, De la Fuente JR, Elsaesser HJ, Brooks DG. Overcoming CD4 Th1 cell fate restrictions to sustain antiviral CD8 T cells and control persistent virus infection. *Cell Rep*. 2016;16(12):3286–3296.